CGMS XXXII NOAA-WP-04
Prepared by NOAA
Agenda Item: B.4

Anomalies from Solar Events
Status of Solar Cycle 23 and Recent Effects on Technology and Humans

NOAA-WP-04 informed the CGMS that the space weather storms of late October to early November 2003 constituted the highest levels of activity seen to date for solar cycle 23. This high activity interval began with the appearance of three large, complex sunspot Regions which we have discussed in detail in this document. Of these three, Region 486 grew to be the largest sunspot region of the current solar cycle and became the dominant producer of spectacular solar events which also produced significant geophysical consequences.

Among the 17 major flares that were observed during the period, the X17 on 28 October, the X10 on the 29 October, and the X28 on the 4 November and their associated coronal mass ejections stand out as extraordinary. The X17 on the 28^{th} is the 4^{th} largest X-ray flare on record (which begins in 1976) and was followed by a rapid rise in the flux of energetic protons in the geospace environment.

The X10 flare and associated CME of 29 October were also remarkable for their subsequent geophysical effects. The X10 stands as the 20^{th} largest x-ray flare on record. The event was followed by another rapid injection of energetic protons in the geospace environment, producing a secondary maximum up to 3298 PFU at 10 MeV, and prolonging the proton event through early on 31 October.

The X28 flare and fast CME on 4 November were an incredible finale for Region 486 as it transited the West limb. The x-ray flare is very likely the largest observed during the GOES/SMS observing era of the past 28 years and the CME speed of about $2.4x10^3$ km/s is truly an extreme.

A wide range of effects on human activities and technological systems were observed. The most extensively reported effects were seen from the interaction of energetic particles with human spacecraft operations and in spacecraft electronics difficulties. NOAA discussed a number of specific deep space missions and near-earth satellites which were affected. Perhaps of greatest significance are the loss of the MARIE instrument on the Mars Odyssey mission and the loss of the ADEOS-2 satellite (which had about development cost of about $640 million). The impact of this interval on airline operations is also particularly noteworthy. Airline routes and schedules were significantly affected because of communication degradation in the daylit and Polar Regions and because of concerns about increased radiation exposure in the Polar Regions.

Although the spacecraft and the airlines effects were most prevalent, it is also clear that a broader range of problems occurred, including HF/VHF communication systems, LF/VLF communications, Global Positioning System (GPS) applications, and electrical power systems. The disruption of electrical power in southern Sweden for about 30 minutes during the activity late on October 30th is certainly a significant example.

What makes this interval of activity particularly noteworthy from a scientific and technical point of view is the diversity of space weather observations which were being made, many of which were not available in the past during similar extreme space weather events. The high levels of geophysical impacts and the wide range of observations will undoubtedly lead to more detailed and extensive analyses of space weather then have been possible in the past.

Anomalies from Solar Events
Status of Solar Cycle 23 and Recent Effects on Technology and Humans

Introduction

Solar Cycle 23 is now more than three years past maximum, and well into its declining phase. Sunspot numbers, 10.7 cm solar flux, and other indicators are reinforcing the opinion that Cycle 23's maximum era is over. This calming behavior should continue to mid 2007, projected to be the next solar minimum. However, the Sun still continues to produce significant space weather as illustrated by the Halloween space weather storms of 2003. Highlights of those storms are discussed later in this paper.

Generally, the more explosive types of activity - solar flares and coronal mass ejections - are mostly less frequent and impressive, the Sun still affects Earth's magnetosphere with yet another type of stimulus - the high-speed solar wind. During the decline of the cycle, the solar magnetic field organizes itself in a way that supports long-lived coronal holes - density voids with open magnetic field topology in the outer solar atmosphere - that allow for the unimpeded escape of the solar wind from the Sun. This fast solar wind, with its embedded magnetic field, energizes Earth's magnetosphere. A consequence of the prolonged episodes of fast solar wind is large quantities of energetic (>2 MeV) electrons now occurring at geosynchronous orbit. These electrons can have a serious, deleterious impact, on satellites in orbit there. Energetic electrons cause deep dielectric charging of satellites, and can ultimately end the service life of a spacecraft. Serious satellite problems in 1994, 1996 and again in 1997 - at relatively the same point in the solar cycle - were diagnosed to be due to the cumulative impact of energetic electrons.

Space weather continues to affect many space-based, as well as earth-based, technologies. Emerging applications are finding that, even in the decline of the activity cycle, space weather is a significant factor for the proper function of their systems.

Solar Cycle Update

Solar Cycle 23 attained its maximum, as measured by sunspot numbers, in April 2000. Recent solar cycle sunspot number amplitudes are given in Table 1 (Thompson, 2002). The smoothed sunspot number of 120.8 fell well short of the predicted maximum of 160. That prediction would have been comparable to the previous two cycles 20 and 21, though well short of the largest ever-recorded maximum of 201 during Cycle 19, observed in April of 1957. Even the "odd-even" rule-of-thumb has been broken. This venerable rule, which says that an odd numbered cycle is larger than the preceding even numbered cycle, has persisted through six pairs of cycles back to Cycle 8/9 around 1850. However, as noted in Table 1, Cycle 23 broke this rule.

Cycle Number	*Date of Cycle Start*	*Date of Cycle Maximum*	*Amplitude (Sunspot Number)*	*Length (Years)*
17	**1933.8**	**1937.4**	**119**	**10.4**
18	**1944.2**	**1947.5**	**152**	**10.1**
19	**1954.3**	**1957.9**	**201**	**10.6**
20	**1964.9**	**1968.9**	**111**	**11.6**
21	**1976.5**	**1979.9**	**165**	**10.3**
22	**1986.8**	**1989.6**	**159**	**9.7**
23	**1996.3**	**2000.3**	**121**	**?**

Table 1: Recent solar cycle parameters.

Figure 1 gives the history, over the past few cycles, of large solar x-ray flare occurrences. Although those events cluster near solar maximum, they do occur at a decreasing frequency at other points in the cycle. Large solar flares can have a serious impact on HF communications. The shading in the figures allows the reader to see the same point in each of the cycles shown. Note the histogram at left, comparing the M Flares from Cycles 21-23, with Cycle 23 being the least productive.

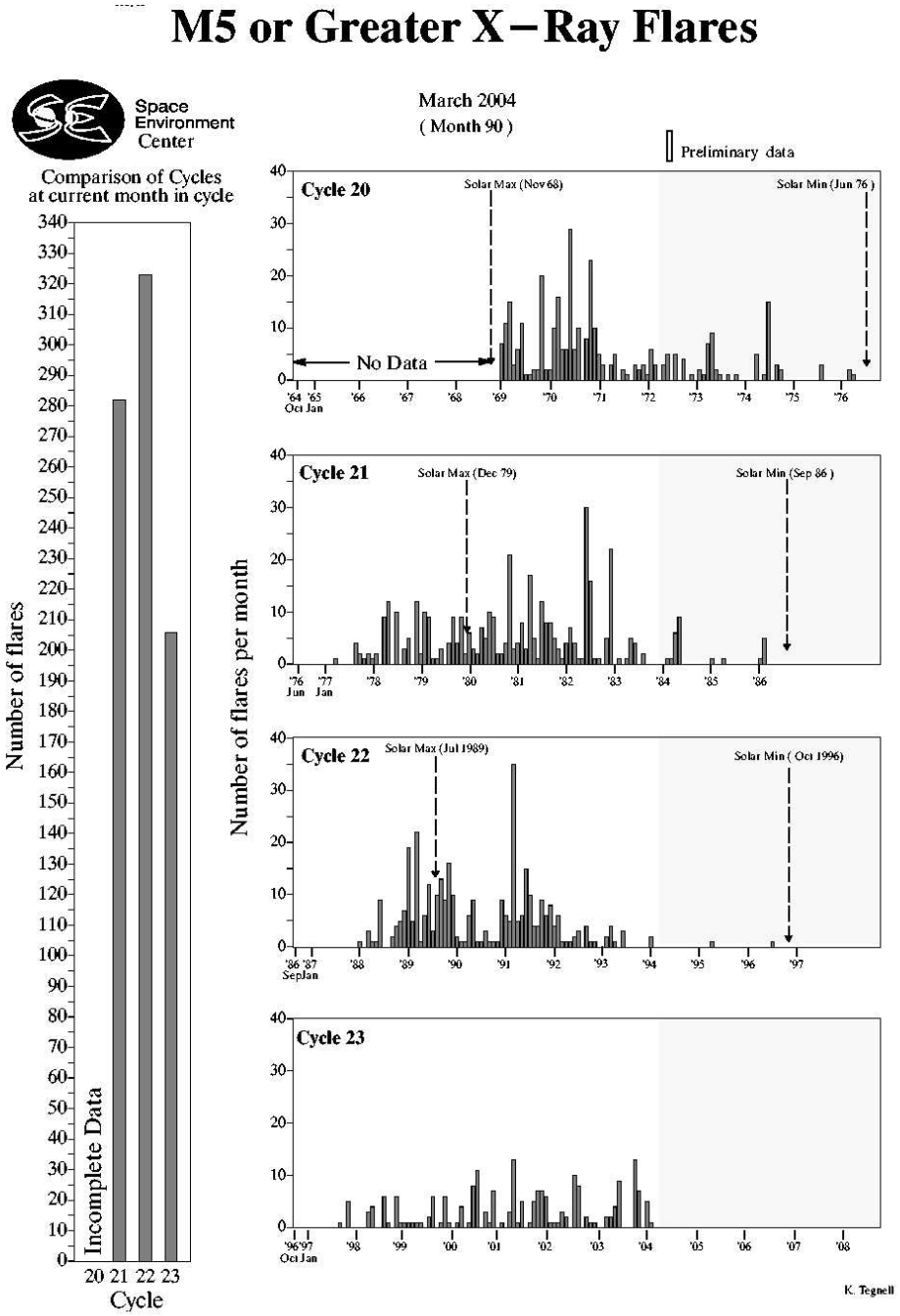

Figure 2 is a summary of geomagnetic activity occurring in Cycles 18-23. Major geomagnetic storm activity shows a bimodal behavior with a secondary peak in the decline of the cycle. This later pulse belies the notion that geomagnetic storms track with the sunspot counts. Cycle 23 was less eventful than all cycles except Cycle 20.

Large geomagnetic activity can significantly affect command and control systems for satellite operation, GPS signals, HF and long-line communications for ground and aviation systems, electric power distribution grids, geophysical exploration and over time, pipeline operations.

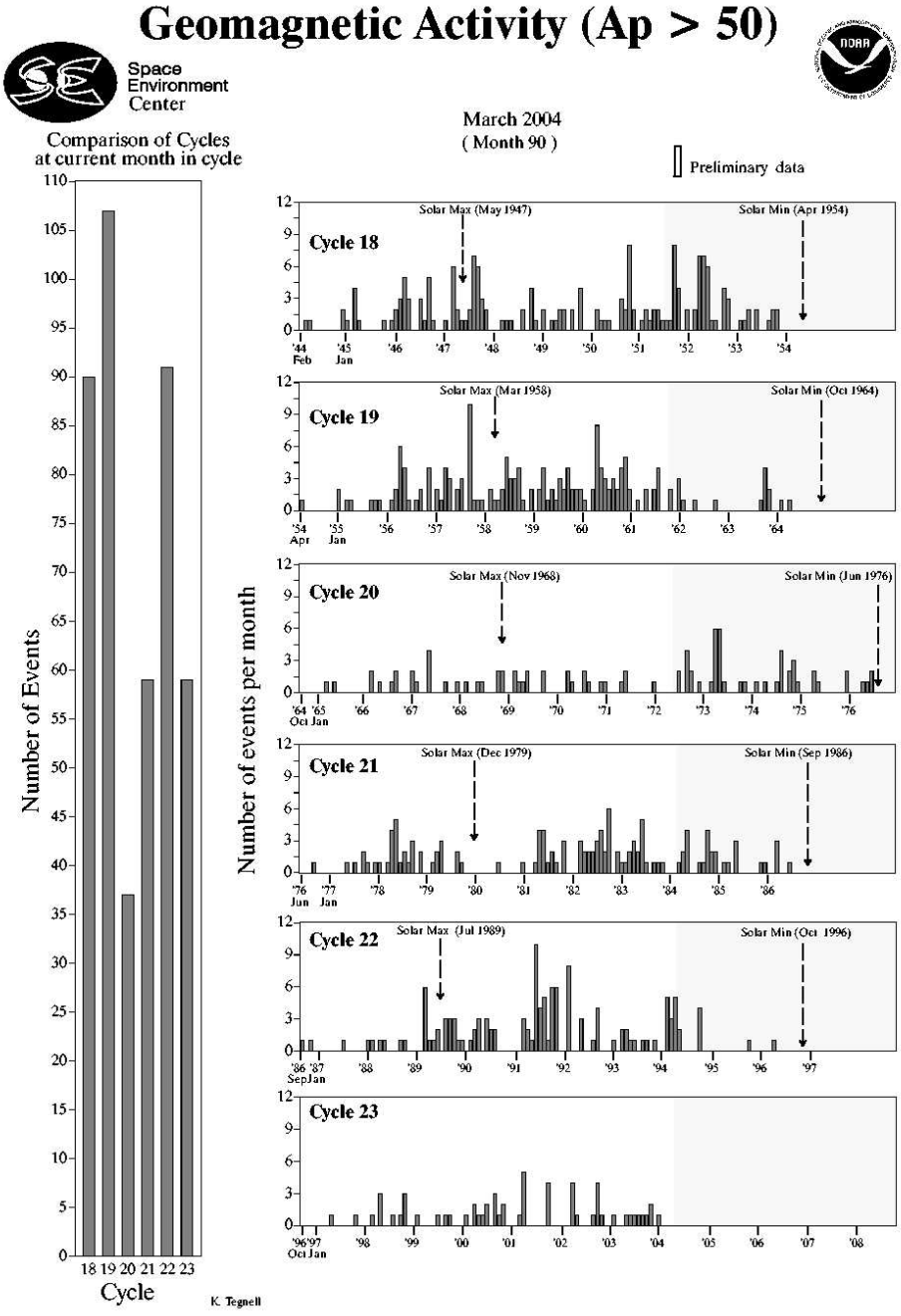

Figure 3 is a summary of the proton events occurring in Cycles 20-23. It is interesting to note that Cycle 23, in terms of the number of events, was the most prolific cycle on record. Proton events have a strong impact on satellite operations, degrading solar panels and interfering with various types of optical systems.

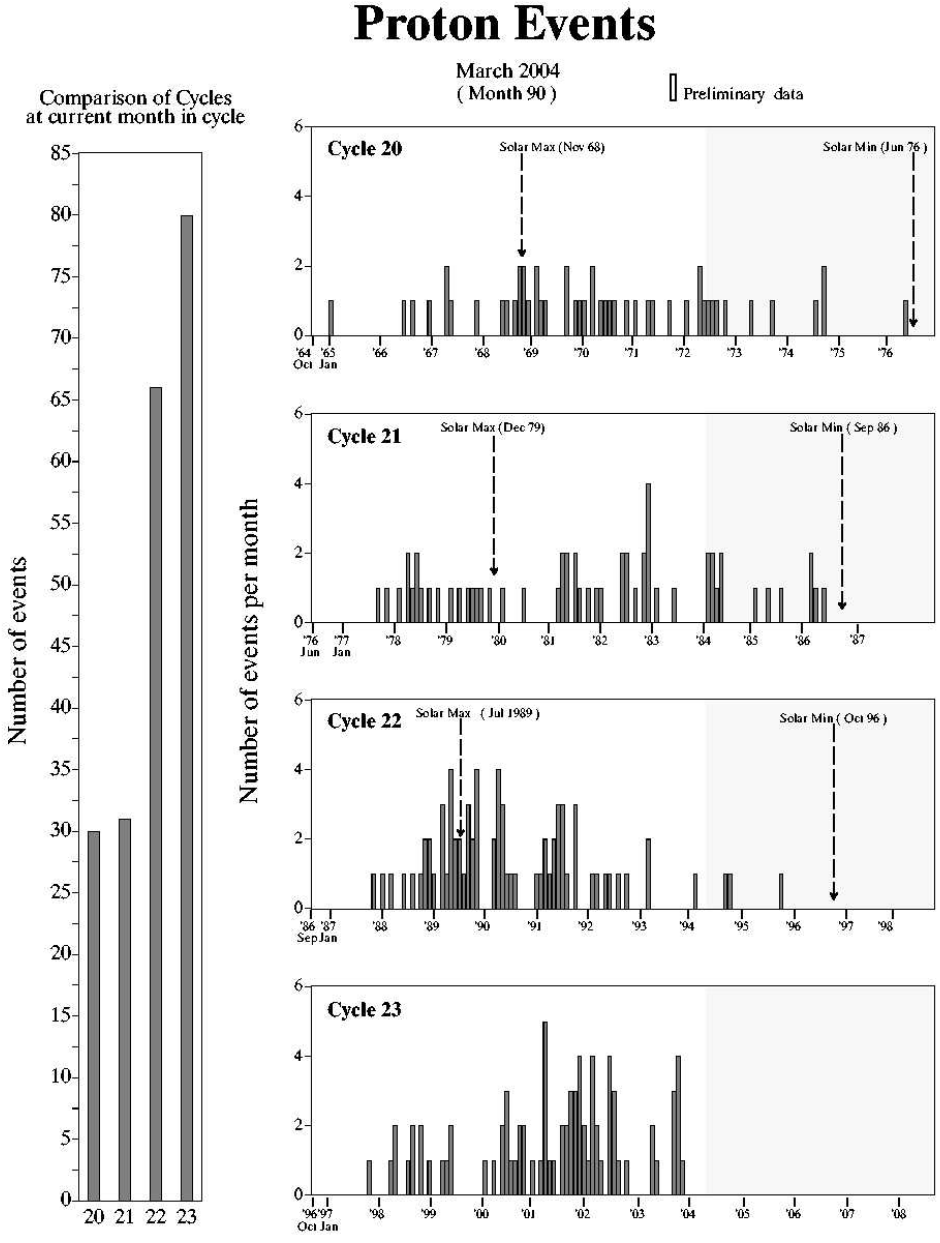

SESC defines Proton Events as periods (in excess of 15 minutes) when the geosynchronous >10MeV proton flux remains above 10 pfu (particle flux unit = 1p/cm*cm*s*sr). Events continue and are counted as a single event until fluxes remain below 10 pfu regardless of whether enhancements from new sources occur. Using different event criteria may result in different event totals.

Halloween Space Weather Storms of 2003

In October and November of 2003, 42 months after Solar Cycle 23's sunspot maximum and well into the declining phase of the cycle, the Sun produced a significant display of solar activity, including one of the largest solar flares ever recorded. The activity produced by the Sun during this period originated from several large and complex sunspot groups. Major solar flare activity was often accompanied by fast Coronal Mass Ejections (CME's) and strong energetic particle events. The arrival of transient solar wind from Earth-directed CME's produced extreme geomagnetic storming. Common effects of these weather phenomena included prolonged HF communication outages, fluctuations in power transmission systems and minor to severe impacts on space satellite systems.

Highlights of the activity observed on the surface of the Sun, the resultant effects in the near-Earth space environment and the impacts to human-made systems in orbit and on Earth follow.

OVERVIEW

Solar Cycle 23 began its approximately 11-year cycle in May 1996 with a monthly smoothed sunspot number (SSN) of 8.0, and peaked in April 2000 at 120.8. The early October sunspot count reflected another quiet month in the unremarkable waning phase of an average solar cycle. The quiet period would abruptly end. In stark contrast, and with little warning, large and intense sunspot groups emerged on the solar surface, and by the end of October 2003, NOAA space weather forecasters were engaged in the most active and demanding solar activity epoch in years. In a 3 week period, staff at the NOAA Space Environment Center (SEC) issued hundreds of space weather watches, warnings, alerts, summaries, and advisories, as the Sun's surface flaunted three of the largest sunspot clusters in over 10 years.

Impacts were wide ranging. Geomagnetically induced currents (GIC) were sufficiently strong over Northern Europe to cause electrical transformer problems and even a power system failure and subsequent blackout in Sweden. Radiation storm levels were high enough to prompt NASA officials to issue a flight directive to the International Space Station (ISS) astronauts to take precautionary shelter. Airlines took unprecedented actions in their high latitude routes to avoid the high radiation levels and communication blackout areas. Numerous anomalies were reported by deep space missions and by satellites at all orbits. Due to the variety and intensity of this solar activity, most industries vulnerable to space weather experienced some degree of impact to their operations.

The activity received intense coverage by media agencies around the world. SEC staff participated in hundreds of news broadcasts and interviews, assisting media representatives from Chile to Hong Kong. The high levels of activity generated more public and media interest than any other solar event or period this cycle. The heightened public awareness produced enormous interest on the SEC webpage, which saw the daily average hit rate of 500,000 rise to over 19 million hits on 29 October. Solar images and solar activity stories were flashed on newspapers around the world, making "space weather" a household term.

This activity occurred 42 months after Cycle 23's peak in April 2000 (based on solar sunspot number). While late cycle active periods have occurred in the past, it is rare to see this level of activity during this stage of the solar cycle. Seventeen major flares erupted on the Sun between 19 October and 5 November, 2003, including perhaps the largest flare ever measured on the GOES XRS sensor – a huge X28 flare, resulting in an R5 – extreme radio blackout, on 4 November (Figure 1). Many of these flares had associated radiation storms, including an S4 (severe) storm on 29 October. There were also several geomagnetic storms, with two of them reaching the G5 (extreme) level on 29 and 30 October. The last occurrence of such late cycle activity was in April and May 1984 during Solar Cycle 21. That period saw a total of nine major flares (between 20 April – 31 May), 52 months after the December 1979 peak of Cycle 21. It should also be noted that 28 major flares occurred in 1973 during the late stages of Cycle 20. Cycle 20 peaked in November 1968. Table 1 Summarizes the activity during this period.

Table 2: Solar Activity Summary															
X-ray Event and Region						**Radio Emissions**			**Coronal Mass Ejections**				**NOAA Scales**		
Flare Max Date Time	Xray Class	Opt Class	Reg	Location	245 Mhz (SFU)	2695 Mhz (SFU)	Ty II Spd. (km/s)	Transit Time (hrs)	Halo Type	Plane of Sky Spd. (km/s)	Shock @ ACE				
19 Oct 1650	X1.1	1n	484	N08E58	650	510	625		P	458		R3		
22 Oct 2007	M9.9	Sf	486	S18E78	100	240						R2		
22 Oct 0351	M3.7	Sf	484	N07E25		320		59.6	F	651	24/1450	R1		G3
23 Oct 0835	X5.4	1b	486	S21E88	10000	1500	967		F	1110		R3		
23 Oct 2004	X1.1	1n	486	S17E84	2500	77						R3		
24 Oct 0254	M7.6	1n	486	S19E72	6800							R2		
26 Oct 0654	X1.2	3b	486	S15E44	14000	4000	1302		P	1245		R3	S2	
26 Oct 1819	X1.2	1n	484	N02W38	1100	2000	950	31.8	F	1432	28/0130	R3		
26 Oct 2140	M7.6	2n	484	N01W38								R2		
27 Oct 0927	M5.0	Sf	486	S16E26	65							R2		
27 Oct 1243	M6.7	Sf	486	S17E25	420	59						R2		
28 Oct 1110	X17.5	4b	486	S16E08	490000	13000	1250	19.0	F	2125	29/0559	R4	S4	G5
29 Oct 2049	X10.0	2b	486	S15W02	360000	2500	775	19.0	F	1948	30/1620	R4	S3	G5
02 Nov 1725	X8.3	2b	486	S14W56	24000	7700	1691	37.0	F	1826	04/0600	R3	S3	G3
03 Nov 0130	X2.7	2b	488	N10W83	100	240	1400		P			R3		
03 Nov 0955	X3.9	Sf	488	N08W77	3900	4400	869		P			R3		
04 Nov 1950	X28.0	3b	486	S19W83	4800	20000	1268	47.8	F	2381	06/1915	R5	S2	G2
05 Nov 1052	M5.3	Sf	486	S16W90								R2		
Note 1								Note 2, 3			Note 1			

Notes:

1. All dates and time are in universal time (UTC).
2. From maximum of X-ray event to the time of sudden impulse.
3. The transit time for the CME associated with the X10 flare on 29 October is estimated since there was no sudden impulse from the shock arrival.
4. Start time of 29/2150 for the 10 MeV proton event is the time of onset of secondary enhancement. The 10 MeV proton event from 28/1215 was still in progress. 10 MeV proton event end time for both events are the same – the time proton levels dropped below the 10 PFU threshold.
5. Start time of 29/2150 for the 100 MeV proton event is the time of secondary enhancement onset. The 100 MeV proton event from 28/1150 was still in progress. 100 MeV proton event end time for both events are the same – the time proton levels dropped below the 1 PFU threshold.

SOLAR ACTIVITY

Solar activity from 19 October to 5 November 2003 originated from three large and complex sunspot regions. SEC Space Weather Operations numbered these sunspot clusters as Region 484, Region 486, and Region 488. While each of these regions was remarkable in size and magnetic complexity, Region 486 was the most significant, growing to become the largest sunspot group of this solar cycle, with a maximum area of 2610 millionths. Of the 17 major flares that occurred during this period twelve were from Region 486, including an X17 on 28 October, an X10 on 29 October, and an X28 (estimated) on 4 November.

X-Ray Flares, Radio Emissions, and LASCO/EIT Observations

Major solar activity began on 19 October as Region 484 rotated around the east limb. A X1 (1n) flare occurred at 1650 UTC near N08E58. Associated with this flare was a Type II radio sweep ($6.3x10^2$ km/s), tenflare, 245 MHz radio burst and other discrete frequency radio bursts. LASCO imagery revealed a partial halo Coronal Mass Ejection (CME) with a plane-of-sky speed measured at $5.5x10^2$ km/s. As Region 486 rotated onto the disk it produced an M9 (Sf) at 2007 UTC on 22 October, near S18E78.

Table 3: Top Flares Since 1976

Rank	*Date*	*X-ray*	*Region*
1	**11/04/03**	**X28e**	**486**
2	08/16/89	X20e	5629
3	04/02/01	X20e	9393
4	**10/28/03**	**X17**	**486**
5	07/11/78	X15e	1203
6	03/06/89	X15e	5395
7	04/24/84	X13e	4474
8	10/19/89	X13e	5747
9	06/06/82	X12e	3763
10	06/01/91	X12e	6659
11	12/15/82	X12	4026
12	06/04/91	X12e	6659
13	06/06/91	X12e	6659
14	06/11/91	X12e	6659
15	06/15/91	X12e	6659
16	12/17/82	X10	4025
17	05/20/84	X10	4492
18	01/25/91	X10	6471
19	06/09/91	X10	6659
20	**10/29/03**	**X10**	**486**

NOTE: Flares with an "e" suffix are estimated due to saturation of the GOES XRS instrument. The saturation level

Region 486 continued to produce major flares on 22-24 October with two X-class flares and an M-class flare. The first of these events was an X5 (1b) flare at 0835 UTC near S21E88, which occurred on 23 October. Significant radio emissions were associated with the event including a Type II radio sweep ($9.7x10^2$ km/s), a 1500 SFU tenflare, and a 10,000 SFU 245 MHz radio burst. EIT and LASCO imagery observed a large EIT wave with dimming and a full halo CME associated with this flare, although the CME was not Earth-directed. A complex filament eruption near Region 484 occurred early on 22 October and produced an Earth-directed CME. This CME is the mostly likely source of the shock and transient flow observed on 24 October, which produced a brief period of severe geomagnetic storming. The second X-class event on 23 October was an impulsive X1 (1n) at 2007 UTC near S17E84. Radio emissions at were observed from this flare including a 2,500 SFU radio burst at 245 MHz. Early on 24 October, Region 486 produced an M7 (1n) at 0254 UTC near S19E72. A Type IV radio sweep and 245 MHz radio burst (6,800 SFU) were associated with this flare. LASCO imagery observed a CME with a plane-of-sky speed of $9.0x10^2$ km/s that was directed off to the east and not towards Earth.

On 26 October, Regions 484 and 486 each produced major flare activity. Region 486 produced an X1 (3b) at 0654 UTC near S15E44. This flare was associated with significant radio emissions including Type II ($1.3x10^3$ km/s) and Type IV radio sweeps, a 14,000 SFU 245 MHz radio burst and a 4,000 SFU tenflare. LASCO imagery indicated an associated partial halo CME with a plane of sky speed measured at $1.2x10^3$ km/s. A large EIT wave and dimming were observed in EIT195 imagery. Later in the day, Region 484 produced an X1 (1n) at 1819 UTC near N02W38. Radio emissions associated with this event included a Type II ($9.5x10^2$ km/s) radio sweep, 1100 SFU 245 MHz radio burst and a 2000 SFU tenflare. A large EIT wave with dimming was observed in EIT imagery and a full halo CME, with a plane-of-sky speed of $1.4x10^3$ km/s, was observed in LASCO imagery. One or both of these events were the likely source of an energetic particle event that began later in the day and a shock that was observed at ACE on 28 October at 0130 UTC. As X-ray levels were declining from the second X1 flare, an impulsive M7 (2n) flare erupted at 2140 UTC from Region 484. No significant radio emissions or CME was associated with this flare.

On 27 October Region 486 produced two M-class events. The first was an impulsive M5 (Sf) at 0927 UTC near S16E26 with only minor radio emissions. The second was an M6 (Sf) at 1243 UTC near S17E25 and was associated with a minor 245 MHz radio burst of 420 SFU.

The most significant solar activity of the late October–early November period began on 28 October. At 1110 UTC, an X17 (4b) flare occurred from Region 486, near S16E08. LASCO imagery revealed an associated, very fast, full halo CME with a plane of sky speed measured at $2.1x10^3$ km/s (see Figure 4). Type II ($1.3x10^3$ km/s) and Type IV radio sweeps were observed as well as a 13,000 SFU tenflare and a 490,000 SFU 245 MHz radio burst. The 245 MHz burst reached the instrumentation limit and was probably higher. EIT imagery indicated a large EIT wave with significant dimming. The event was promptly followed by an energetic 10 MeV proton event that exceeded the 1,000 PFU level within an hour and the 10,000 PFU level within 13 hours. The CME-driven shock arrived at Earth on 29 October at 0613 UTC in just 19 hours. The geomagnetic storm that followed reached extreme (G5) levels and lasted for 27 hours.

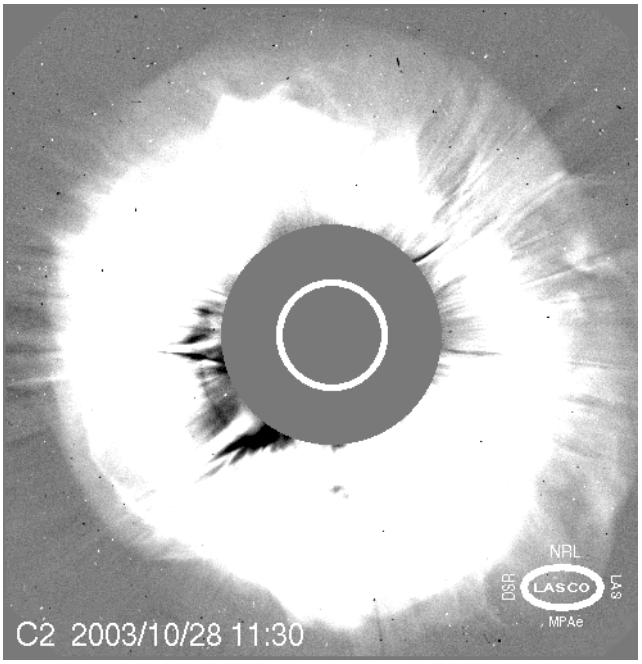

Figure 4: Full halo CME from X17.4 flare on LASCO imagery, 28 October 2003. (Image courtesy of NASA)

Region 486 produced another significant major flare on 29 October. An X10 (2b) flare erupted at 2049 UTC from near S15W02. This flare was also associated with strong radio emissions that included Type II ($7.8x10^2$ km/s) and Type IV radio sweeps, a 360,000 SFU 245 MHz radio burst and a 2,500 SFU tenflare. EIT imagery revealed a large wave and significant dimming. LASCO imagery showed a very fast full halo CME associated with this flare. The plane of sky speed was measured at $1.9x10^3$ km/s, representing

another extremely fast CME. The transit time for this CME was 19 hours, arriving at Earth at 1600 UTC on 30 October. The geomagnetic storm from this CME lasted for 24 hours and reached extreme levels. At the time of this flare a proton event was still in progress due the X17 flare on the 28 October, but the flux was on the decline when the X10 flare occurred. The X10 flare produced a secondary enhancement of energetic protons, as detailed later in this report.

Activity was relatively quiet until 2 November when Region 486 continued with more major flares. An X8 (2b) occurred at 1725 UTC near S14W56. Strong radio emissions were associated with this event: Type II ($1.7x10^3$ km/s) and Type IV radio sweeps and a 24,000 SFU 245 MHz radio burst and a 7,700 SFU tenflare. EIT imagery indicated a very large wave and dimming. LASCO imagery indicated a full halo CME, with a plane of sky speed measured at $1.8x10^3$ km/s. The geomagnetic response was observed at Earth around 0630 UTC on 4 November as a brief geomagnetic storm.

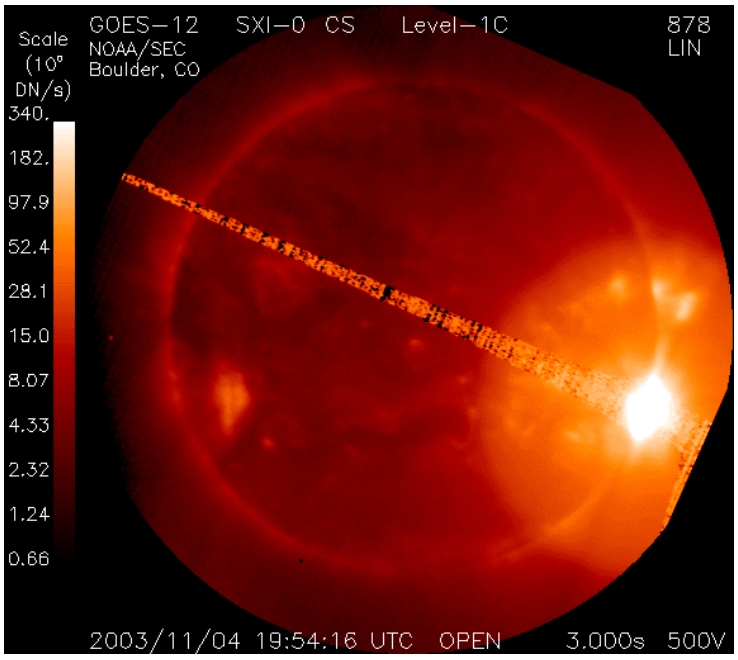

Figure 5: GOES SXI Imagery of the X28 (estimated) flare on 4 November 2003.

Region 488 produced two major flares near the end of its disk passage on 3 November. The first flare was an X2 (2b) at 0130 UTC near N10W83. Radio emissions included Type II ($1.4x10^3$ km/s) and Type IV radio sweeps as well as a minor 245 MHz radio burst and tenflare. LASCO imagery showed a partial halo CME in the northwest associated with the X2 flare. The second major flare from Region 488 was an X3 (Sf) at 0955 UTC near N08W77. A Type II ($8.7x10^2$ km/s) and Type IV radio sweep were associated with the X3 flare as well as a 3,900 SFU 245 MHz radio burst and a 4,400 SFU tenflare. LASCO imagery indicated a partial halo CME off the northwest limb.

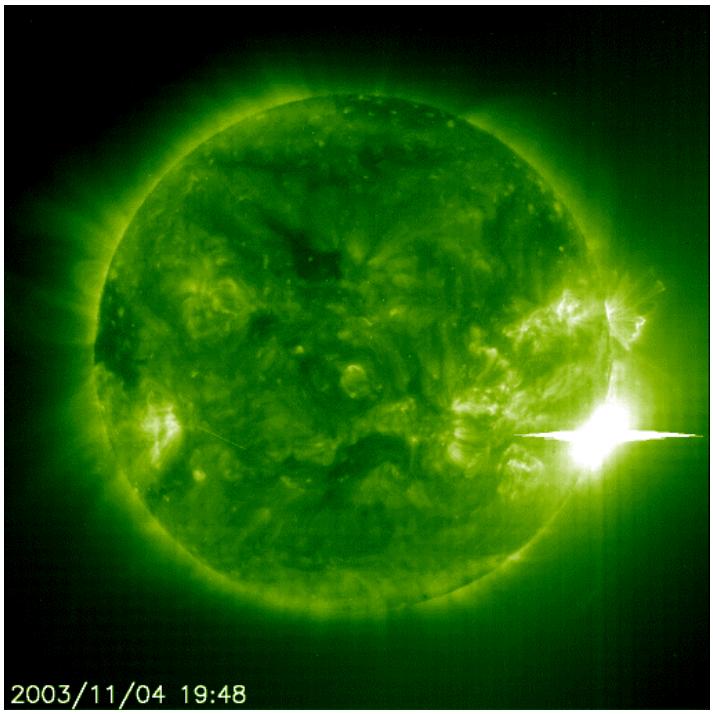

Figure 6: SOHO/EIT Imagery of the X28 (estimated) flare on 4 November 2003. (Image courtesy of NASA)

The last event of significance during the October-November period of activity was an X28 (estimated) major flare from Region 486 (Figures 5 and 6). The X28 (3b) flare occurred on 4 November at 1950 UTC near S19W83. The GOES XRS instrument used to measure X-ray emissions became saturated at the X17.5 level for 12 minutes during this flare. Using historical flare data and mathematical modeling the peak flux was estimated to be X28. This flare may be the largest flare observed since 1976 when GOES X-ray measurement of solar flares began, although there are other flares in the record which also saturated the sensor. Radio emission from this flare included Type II ($1.3x10^3$ km/s) and Type IV radio sweeps and a 4,800 SFU radio burst at 245 MHz and a 20,000 SFU tenflare. EIT 195 imagery showed a very large wave and significant dimming. LASCO imagery indicated an associated full halo CME, measuring a plane of sky speed of $2.4x10^3$ km/s (Figure 7). Despite the record size of the flare and high speed of the CME, its location near the west limb of the Sun limited its impact at Earth. The center of the CME was directed off the northwest limb and away from Earth and was observed as a glancing blow at Earth. The transient flow produced minor storm conditions for a brief 3 hour period on 6 November. A moderate proton event was associated with this flare, lasted for about 3 days, and ended late on 7 November.

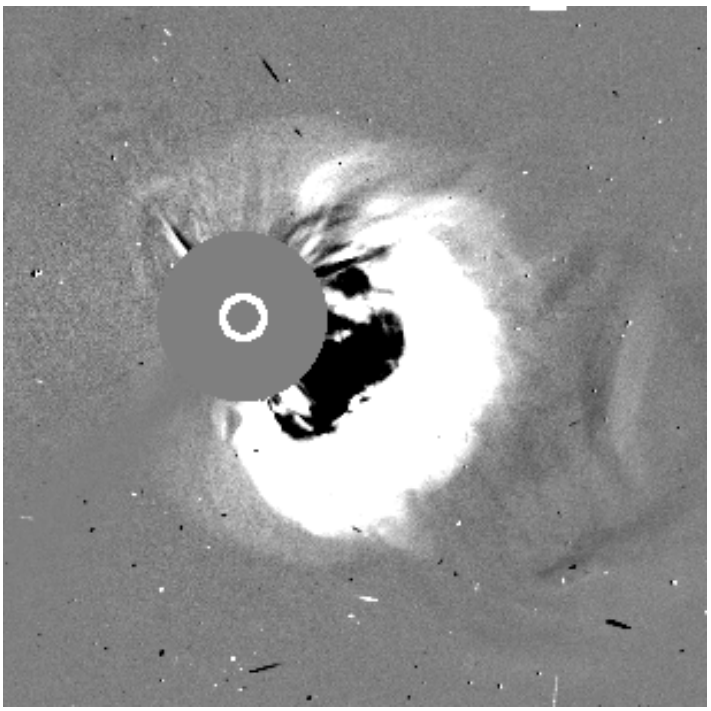

Figure 7: Full halo CME from X28 (estimated) flare on LASCO imagery on 4 November 2003. (Image courtesy of NASA)

The last major flare of the period was an impulsive M5 (Sf) that occurred at 1052 UTC on 5 November. This flare was located on the southwest limb and Region 486 was the most likely source. No significant radio emissions or CME's were associated with this event.

GEOPHYSICAL EVENTS

a. Solar Proton Events

The high space weather interval from 19 October to 7 November 2003 included four separate energetic proton events, including the fourth largest proton event at 10 MeV on record (Table 4). Two of these events were complex, consisting of multiple injections of energetic particles from separate sources, which led to multiple maxima within the events. These particle events were particularly noteworthy because of the widespread, significant effects they caused on a number of spacecraft (see Section 5 for details).

Table 4: Top Radiation Storms Since 1976

Rank	Peak Intensity (PFU)	Date
1	43,000	23/03/1991
2	40,000	19/10/1989
3	31,700	04/11/2001
4	**29,500**	**28/10/2003**
5	24,000	14/07/2000
6	18,900	22/11/2001
7	14,800	08/11/2000
8	12,900	24/09/2001
9	10,000	20/02/1994
10	9,200	12/08/1989
11	7,300	30/11/1989
12	4,600	09/05/1982
13	4,500	29/09/1989
14	3,500	08/03/1989
15	3,000	04/06/1991
16	2,900	11/06/1982
17	2,700	30/10/1992
18	2,520	21/04/2002
19	2,500	25/04/1984
20	2,360	01/10/2001

The first event began at 1825 UTC on 26 October. Although there was some ambiguity about the solar origin of this event, the most likely candidate is the X1 flare from Region 486, which occurred on 26 October at 0654 UTC when the region was located at S15E44. The 10 MeV protons began their rise approximately 11 hours after this maximum. The proton event maximum was 465 PFU at 2235 UTC. The event ended on 27 October at 0820 UTC. There was a small enhancement of the 100 MeV protons; however, the flux did not exceed the SEC alert threshold of 1 PFU.

The X17 flare from Region 486, which was centered at S16E08 on 28 October at 1110 UTC, produced both 10 MeV and 100 MeV proton events. The 10 MeV protons rose abruptly after the maximum of the flare, with the event beginning at 1215 UTC. The 10 MeV proton event maximum was 29,525 PFU at 0615 UTC on 29 October. This event is the fourth largest proton event on record. The X17 flare also produced a 100 MeV proton event, which began 5 minutes after the maximum of the flare, and reached event level at 1145 UTC on 28 October. This 100 MeV proton event reached a maximum of 185 PFU on 29 October at 0015 UTC (Figure 18).

There was a secondary 10 MeV proton enhancement that originated from an X10 flare from Region 486, which was centered at S15W02 on 29 October at 2049 UTC. There was already a 10 MeV event in progress at the time of this event. However, the onset of new particles from the X10 event is clearly observed at about 2100 UTC. This enhancement produced a secondary maximum of 3298 PFU on 30 October at 1935 UTC. The greater than 10 MeV proton event finally dropped below threshold on 1 November at 1055 UTC. The X10 flare also produced a secondary enhancement in the 100 MeV protons. The enhancement produced a secondary maximum of 109 PFU on 29 October at 2310 UTC. The greater than 10 MeV proton event ended on 31 October at 0145 UTC.

An M3 flare from Region 486 centered at S12W60 on 1 November at 2238 UTC produced a comparatively small 10 MeV proton event. The event began on 2 November at 1105 UTC and reached a maximum of 30 PFU on 2 November at 1415 UTC.

There was a secondary 10 MeV proton enhancement that was due to an X8 flare from Region 486 centered at S14W56 on 2 November at 1725 UTC. A 10 MeV proton event was already in progress when a rise was seen on the GOES-11 particle channels at about 1730 UTC. The rise was almost simultaneous with the maximum of the flare. This enhancement led to a secondary maximum of 1518 PFU on 3 November at 1345 UTC. The entire 10 MeV proton event then ended on 4 November at 2120 UTC. The X8 also produced a 100 MeV proton event. The event began on 2 November at 1740 UTC, reached a maximum of 49 PFU at 1905 UTC, and ended on 3 November at 1720 UTC.

The last 10 MeV proton event was from the X28 flare that occurred on 4 November at 1950 UTC from Region 486 centered at S19W83. The 10 MeV proton flux began to rise 2 hours 20 minutes after the maximum of the flare. The event threshold was crossed on 4 November at 2225 UTC and the event reached a maximum of 353 PFU on 5 November at 0600 UTC. This event then began a very gradual decline, finally ending on 7 November at 2115 UTC. The X28 produced a very gradual rise in the 100 MeV proton channel. The event took 3 hours 20 minutes from the time of flare maximum to begin to rise. The event threshold was crossed on 5 November at 0535 UTC, and maximum flux of 1 PFU was reached at 0540 UTC. The 100 MeV event ended at 0705 UTC.

b. Geomagnetic Storms

There were three separate geomagnetic storms during the period 19 October thru 7 November 2003. These included the sixth and sixteenth largest geomagnetic storms recorded based on the 24 hour running Ap index (Table 5). The arrival times for two of the storms were unusually fast, under 20 hours.

Table 5: Top 30 geomagnetic storms based on Potsdam running A_P

Rank	A_P	Date
1	312	09/18/1941
2	293	11/12/1960
3	285	03/13/1989
4	277	03/23/1940
5	258	10/04/1960
6	**252**	**10/29/2003**
7	252	07/15/1959
8	251	03/31/1960
9	241	05/25/1967
10	229	07/11/1982
11	228	02/07/1986
12	226	03/29/1940
13	223	08/04/1972
14	222	07/05/1941
15	221	09/02/1957
16	**220**	**10/30/2003**
17	216	07/08/1958
18	215	03/28/1946
19	214	09/22/1946
20	212	03/01/1941
21	212	07/26/1946
22	203	08/19/1950
23	201	09/04/1982
24	199	02/07/1946
25	199	02/11/1958
26	196	05/12/1949
27	196	06/04/1991
28	195	03/24/1946
29	193	05/09/1992
30	192	07/14/2000

24 – 25 October 2003

The storm that began on 24 October was not as impressive as the other storms that were to follow in this activity period. This storm began with a 105 nT sudden impulse (SI) observed at Boulder on 24 October at 1529 UTC. Geomagnetic storming occurred nearly 30 hours after the maximum time of the associated flare. The highest Kp observed during the storm period was a Kp=7- observed 24 October between 1500 and 1800 UTC. This storm could have been stronger; however, the interplanetary field observed at ACE remained mostly northward and only a single period of Kp=7- was observed. The highest 24 hour running Ap for this storm was from 24 October at 0900 UTC to 25 October 0900 UTC and was 43. The actual storming period lasted 12 hours and ranged from minor to severe storm levels.

29 – 30 October 2003

29 thru 30 October produced the sixth largest geomagnetic storm on record since 1932, based on the running Ap index. The CME that drove this storm took approximately 18 hours 45 minutes to reach Earth. A 140 nT sudden impulse was observed at Boulder on 29 October at 0613 UTC. Subsequent to the SI, geomagnetic activity quickly transitioned to storm levels, with a $Kp=9_0$ (extreme storm) threshold being reached at 0839 UTC. During the storm's duration, major to severe storm levels were observed for a full 24 hour period. The storm's total duration was approximately 33 hours and ranged from minor to severe storming. The running Ap from 29 October 0900 UTC to 30 October 0900 UTC was 252. Table 5 shows that this storm ranks as the sixth largest recorded.

30 – 31 October 2003

This storm began subsequent to the 29-30 October storm after an approximately 3 hour lull in geomagnetic activity. The storm began approximately 19 hours after the maximum of an associated X10 flare on 29 October at 2049 UTC. Planetary indices indicated severe storm levels ($Kp=9_0$) for 6 hours. The highest 24 hour running Ap was 220.

CUSTOMER SUPPORT AND IMPACTS

SEC's customer base is wide ranging and includes multiple agencies involved in deep space missions, satellite and space operations in near-Earth orbits, the airline industry, electric utilities, communications and navigation interests, and more. Support provided by SEC during the high solar activity period differed considerably from user to user. The following section will address the impact of space weather on the various technologies both on Earth and in space and the support provided by SEC to assist these users.

a. NASA Human Spaceflight and International Space Station

The NASA Space Radiation Analysis Group (SRAG) at the Johnson Space Center (JSC) is responsible for ensuring that the radiation exposure received by astronauts remains below established safety limits. Telephone briefings between SEC and SRAG are conducted daily, and the support tempo increases significantly during special operations such as space shuttle missions and extra-vehicular activity (space walks) and during periods of high solar activity. The extensive coordination between SEC and NASA resulted in actions by SRAG that ensured astronauts would not exceed acceptable risk from exposure to radiation, and cut the potential radiation exposure of the crew by approximately 50% by relocating the crew to a more sheltered section of the space station.

NASA also decided to do a ground-commanded power-down of the billion dollar ISS robotic arm and on-board workstation, which are more sensitive to higher than normal radiation events. They prepared to take other precautionary actions (e.g. shut down the S-band antenna controller and external color TV cameras) if radiation levels were to increase more than they did. The ISS Environments System Team also reported that the ISS experienced abnormal frictional drag.

b. NASA Deep-Space Missions

Numerous deep-space missions in progress during the October-November time frame were impacted by the severe solar activity. The lists of impacts below highlight some details of known anomalies.

Mars Odyssey – Spacecraft entered safe mode during the severe radiation storm. During downloading on 29 October, the spacecraft had a memory error that was corrected with a cold reboot on 31 October. The MARIE instrument on the Mars Odyssey had a temperature red alarm which required it to be powered off on 28 October. Recovery is not expected. Ironically, MARIE's mission was to assess the radiation environment at Mars in order to determine the radiation risk for astronauts on a Mars human spaceflight mission.

Stardust – Comet mission went into safe mode due to read errors. The mission has subsequently recovered.

SMART-1 – Spacecraft automatically shutdown the engine due to high radiation levels in lunar transfer orbit. SMART operators reported a total of 3 shutdowns.

Mars Explorer Rover – Spacecraft entered "Sun Idle" mode due to excessive star tracker error events. Operations were suspended during high solar activity and the system subsequently recovered.

Microwave Anisotropy Probe – The spacecraft star tracker reset, and the backup tracker autonomously turned on. The prime tracker has recovered.

Mars Express – The spacecraft had to use gyroscopes for stabilization, because the energetic particle event made it impossible to navigate using stars as reference points. The radiation storm blinded the orbiter's star trackers for 15 hours. The events also delayed a scheduled Beagle 2 checkout procedure.

c. Other Spacecraft

ADEOS-2 – Japan Aerospace Exploration Agency (JAXA) lost contact with the ADEOS-2 satellite, following an intense CME, which impacted Earth's magnetic field on 24 October.
ADEOS-2 is an environmental observation satellite, launched in December 2002 by the Japanese Space Agency. It was designed to collect data on global warming and other climate-change phenomena. The spacecraft was developed at a cost of 70 billion yen ($640 million), and it had an expected lifespan of three years. Recovery is not expected.

Advanced Composition Explorer (ACE) – EPAM Low Energy Magnetic Spectrometer (LEMS 30) was damaged: Noise levels increased in several ion channels and remain abnormally elevated. Recovery is not expected.

Kodama, Data Relay Test Satellite (DRTS) – The spacecraft went into safe mode on the morning of October 29, during the severe (S4) solar radiation storm. The DRTS is a geostationary communications satellite that relays data among Low Earth Orbit (300-1,000 km altitude) spacecraft (including the International Space Station) and ground stations. Kodama was recovered on 7 November at 2119 JST.

CHIPS – The satellite computer went offline on 29 October and contact was lost with the spacecraft for 18 hours (loss of 3-axis control because its Single Board Computer (SBC) stopped executing). When contacted, the spacecraft was tumbling, but recovery was successful. It was offline for a total of 27 hrs.

DMSP F16 – The SSIES sensor lost data twice, on 28 October and 3 November. The sensor was recovered. The microwave sounder lost an oscillator. A switch to a redundant system was required to resume operation.

CHANDRA – Observations were halted on several occasions during the high solar activity, including an extended outage from 28 October to 1 November.

GOES-8, 9, 10 and 12 – The spacecraft experienced high bit error rates (9 and 10) and magnetic torquers were disabled (12) due to solar activity. The GOES-8 X-ray Sensor turned itself off and could not be recovered.

Inmarsat (fleet of 9 geosynchronous satellites) – Controllers at its Satellite Control Centre had to quickly react to the solar activity to control Inmarsat's fleet of geosynchronous satellites. Two

satellites experienced speed increases in momentum wheels which required firing of thrusters to mitigate. One satellite had an outage when its CPU went offline.

TV and Pay Radio Satellite Services: TV satellite controllers reported many problems with maintaining routine operations. They had to resort to "manual attitude control" for 18 hour to 24 hour periods due to magnetopause crossing events that affect the attitude controller of two or more of their fleet. A component has "burned out" in one circuit box in a newer satellite. The failure required a workaround which was successful. Pay radio satellite had several short-lived periods when they lost satellite signal lock.

d. Mitigating Actions Taken by Spacecraft Operations Teams

Aqua, Landsat, Terra, TOMS, TRMM – NASA's Earth Sciences Mission Office directed all instruments on these five spacecraft be turned off or safed due to a Level 5 storm prediction (29 October).

SIRTF – In orbit while drifting behind Earth, operators turned the science experiments off due to high proton fluxes (29 October). Four days of operations were lost.

The **CDS** instrument on **SOHO** spacecraft was placed into Safe mode for 3 days (28-30 October).

UARS/HALOE – The activation of the instrument was delayed due to activity.

e. Global Positioning System (GPS)

GPS operations are affected by changes in total electron content (TEC) of the ionosphere along the path to the satellite during large flares and geomagnetic storms. Significant storms can cause large increases and decreases in TEC, which impact the accuracy of single-frequency GPS. Dual-frequency GPS receivers can better adjust to a disturbed ionosphere, but still experience some degraded signals and position errors.

Many GPS users will experience little or no impact during TEC disturbances, but those requiring precise GPS measurements have a great need for SEC alerts and warnings. Those with the greatest concerns include surveying companies using GPS measurements for land surveying, topographic work, and property boundary analysis, deep-sea drilling operations, land drilling and mining, and various DoD operations.

Operators relying on GPS can and will take important actions during geomagnetic storms. During the October-November activity, companies delayed high resolution land surveying, postponed airborne and marine survey operations, cancelled drilling operations, and some, as was the case with the C.R. Luigs deep water drill ship, resorted to backup systems to ensure continuity of operations.

f. Airline Operations

Airlines have long recognized the potential cost benefits of flying polar routes for flights from North America to Asia. The end of the Cold War opened these flight paths and by the end of the last decade, several airlines were operating on these new shorter and efficient routes. Airlines using polar routes benefit from additional passenger revenue, while producing significant savings on fuel and crew costs. Typical time and cost savings for a New York to Singapore flight is 209 minutes and $44,000; The Boston to Hong Kong polar flight will save 138 minutes and $33,000.

The polar routes are impacted significantly by solar activity. Airlines on polar routes must contend with degraded communications; potential biological impacts from radiation storms; impacts to navigational systems (generally a lesser concern); and as avionics evolve, a potential impact to electronic systems. The October-November solar storms created a significant disruption to airline operations. Some polar flights were diverted, requiring additional stop-offs and resulting in additional fuel, flight time, and also costly crew exchanges.

HF/VHF Communications

Polar flights departing from North America use VHF (30-300 MHz) communication with Canadian Air Traffic Control (ATC) and Arctic Radio. When at high latitudes outside of the range of VHF, aircraft communicate via HF (3 – 30 MHz). Satellite Communications (SATCOM) is considered a backup during polar flights, but it is rarely available above 82 degrees North Latitude. Airlines and ground controllers experienced communications problems from 19-23 October, but these initial HF communication blackouts were short-lived and limited to the sunlit side of Earth. The first significant impact to airline operations occurred on 24 October 2003 following the onset of a G3 (strong) geomagnetic storm. Solar radiation remained at background levels, but high-latitude communications were severely degraded due to the geomagnetic storm. These communication problems forced the Edmonton Air Traffic Control Center to release notices to airmen (NOTAM) and place some restrictions on airline operations in high-latitudes.

This was the first of several such periods of severely degraded communication. As each major flare occurred, HF communications at low and mid-latitudes underwent a range of problems from minor signal degradation to complete HF blackout. Higher latitudes experienced additional difficult periods following the onset of the radiation storms on 26 October.

Space Radiation Effects

Essentially all commercial aviation interests were made aware of the radiation storm levels on 28-29 October, when the Federal Aviation Administration (FAA) issued their first ever advisory suggesting that airline pilots stay below 25,000 feet when traveling above 35 degrees latitude, both north and south. This FAA product is based on the NOAA GOES particle sensors and is advisory only. Airlines are not required to take action based on this advisory. Several flights on the U.S. to Europe routes did fly at lower altitudes during this severe radiation storm. The FAA issued a Solar Radiation Alert for the following timeframes:

Start	End	Duration
10/28 1208 UTC	10/29 0603 UTC	17h 55min
10/29 2123 UTC	10/30 1158 UTC	14h 35min
11/02 1808 UTC	11/02 2343 UTC	05h 35min

```
Space Weather Message Code: ALTPAV
Serial Number:  1006
Issue Time: 2003 Oct 28 2123 UTC

ALERT: Solar Radiation Alert at Flight Altitudes
Conditions Began: 2003 Oct 28 2113 UTC

Comment:
Satellite measurements indicate unusually high levels of
ionizing radiation, coming from the sun. This may lead to
excessive radiation doses to air travelers at Corrected
Geomagnetic (CGM) Latitudes above 35 degrees north, or south.

Avoiding excessive radiation exposure during pregnancy is
particularly important.

Reducing flight altitude may significantly reduce flight
doses. Available data indicates that lowering flight altitude
from 40,000 feet to 36,000 feet should result in about a 30
percent reduction in dose rate. A lowering of latitude may
also reduce flight doses but the degree is uncertain.  Any
change in flight plan should be preceded by appropriate
clearance.
```

Figure 8 – Text of the FAA Solar Radiation Alert issued on 28 October 2003

Some airlines have established their "go/no-go" radiation storm threshold at the S3 level. Dispatchers informed SEC that they must make route decisions several hours in advance of the scheduled takeoff time and that a prediction of a storm being above or below the S3 level is vital. Maximum intensity predictions are not part of SEC's routine radiation storm warning products. Forecasters adjusted to this need and provided dispatchers with radiation storm maximum intensity predictions. Perhaps the best example of the value of a maximum intensity prediction was on 4 November, when the X28 (R5 extreme) flare erupted. Some airlines immediately assumed a flare this large would produce a significant radiation storm. Forecasters advised dispatchers that because of the source location on the Sun, an S3 storm was unlikely. No route alterations were made, and the prediction was vindicated when a moderate size S2 radiation storm unfolded.

g. Antarctic Operations

The Antarctic science groups and staff rely on a company called MacRelay to provide essential radio communications between McMurdo Station and remote sites on the Antarctic. MacRelay is also responsible for communication links with aircraft and ships supporting the United States Antarctic Program. The primary source of communication is HF radio. MacRelay experienced over 130 hours of HF communication blackout during the October – November activity.

Following an extended solar flare induced HF outage earlier in this solar cycle, McMurdo staff developed a contingency plan to use Iridium satellite phones as backup during HF outages. During the previous periods of severe solar activity, numerous support flights were delayed for several days, since take-off and landing restrictions are increased during HF blackouts. The LC-130 aircraft that service the remote sites use Iridium phones to communicate with McMurdo and the remote locations.

Scientific missions in the field (at camp) in Antarctica are required to 'check in' with MacRelay communications under normal circumstances via HF. If they miss their 'check in' then a rescue mission is considered. MacRelay was made aware that space weather was causing an HF blackout conditions, allowing them to implement contingency plans.

h. Electric Utilities

The geomagnetic storms on 29 and 30 October were certainly among the strongest this cycle. When a geomagnetic storm is in progress, the fluctuations of the geomagnetic field induce electric fields and this can drive potentially damaging geomagnetically induced currents (GIC) in electrical power lines and transformers. The late October storms caused GIC's that impacted power grids around the globe.

Typically, when smaller, less powerful storms occur, GIC's at a few Amperes to a few tens of Amperes can cause some problems for grid operators. Larger storms can generate GIC's of well over 100 Amperes which can lead to transformer saturation, over-heating, false relay trippings, an increase of harmonics, voltage depression, and – in worst case scenarios – a blackout of an entire power grid or permanent damage to transformers.

Power companies in North America experienced some problems during the October-November high solar activity. Impacts and actions reported by grid operators included less use and switching between systems, high levels of neutral current observed at stations throughout the country, a capacitor trip in the northwest (known to be GIC susceptible), and transformer heating in the Eastern U.S. Precautions were implemented. For example, a 'growling' transformer was backed down to help cool it. GIC impacts were more significant in Northern Europe where heating in a nuclear plant transformer was reported and a power system failure occurred on 30 October in Malmo, Sweden resulting in blackout conditions for about one hour.

Electrical companies took considerable efforts to prepare for and be aware of the storm onsets. Companies received the standard suite of geomagnetic storm watches, warnings and alerts, but SEC staff also supplemented standard support with several phone discussions. Preventive action helped to counter the GIC stresses that were observed. A representative from the North American Electric Reliability Council (NERC) commented: "Although the bulk electric system was not significantly affected by the solar activity, some systems reported higher than normal GIC's that resulted in fluctuations in the output of some generating units, while the output of other units was reduced in response to the K-index forecast." Responses to warnings included reducing system load, disconnecting system components, and postponing maintenance.

In spite of the high level of solar and geophysical activity during this period, the magnetic storm coupling was considerably less than it could have been and the resultant geomagnetically induced currents were not as large as those observed in the past. According to John Kappenman of the Metatech Corporation, both storms were "far less severe than a Superstorm status and resulting GIC's that did occur could perhaps be a factor of 3 to 10 times larger in most regions than those observed." GIC's in excess of 100 Amps were observed and Kappenman suggested that larger GIC's were observed globally during the large shock on 29 October, following the arrival of the first large CME from the X17 flare (Kappenman, 2003).

i. Aurora

The Aurora Borealis and Aurora Australis (northern and southern lights) are the visible manifestation of geomagnetic disturbances. With the advent of the Internet and other advances in communications, entrepreneurs are seizing commercial opportunities to provide aurora alerts, image galleries and photo sales, and even aurora viewing tours. The public's interest in aurora viewing generated numerous contacts from media and the general public.

Though not a part of SEC's product line, SEC staff assisted with numerous inquiries about aurora viewing. The extreme and prolonged geomagnetic storms on 29 and 30 October ensured widespread middle and even low latitude aurora. Aurora sightings occurred from California to Houston to Florida. Tremendous aurora viewing was also reported from mid-Europe and even as far south as the Mediterranean countries.

SUMMARY

The space weather storms of late October to early November 2003 constitute the highest levels of activity seen to date for solar cycle 23. This high activity interval began with the appearance of three large, complex sunspot Regions which we have discussed in detail in this document. Of these three, Region 486 grew to be the largest sunspot region of the current solar cycle and became the dominant producer of spectacular solar events which also produced significant geophysical consequences.

Among the 17 major flares that were observed during the period, the X17 on 28 October, the X10 on the 29 October, and the X28 on the 4 November and their associated coronal mass ejections stand out as extraordinary. The X17 on the 28th is the 4th largest X-ray flare on record (which begins in 1976) and was followed by a rapid rise in the flux of energetic protons in the geospace environment. The proton flux continued to rise as a fast interplanetary shock transited from the Sun to the Earth, in about 19 hours, leading to a peak flux of 29,525 PFU at 10 MeV with the arrival of the shock early on 29 October. Based on the peak 10 MeV flux this is the 4th largest proton event observed since the records began in 1976. The arrival of the shock was followed by extreme levels of geomagnetic activity as measured by the planetary Kp/Ap indices and by the global Dst (provisional) index, with maximum Kp values of 9_0, a maximum running Ap value of 252, and a maximum Dst of –363 nT. Based on the running Ap-index this is the 6th largest storm since on record (which dates back to 1932) and based on the provisional Dst this is also the 6th largest storm on record (dating back to 1957).

The X10 flare and associated CME of 29 October were also remarkable for their subsequent geophysical effects. The X10 stands as the 20th largest x-ray flare on record. The event was followed by another rapid injection of energetic protons in the geospace environment, producing a secondary maximum up to 3298 PFU at 10 MeV, and prolonging the proton event through early on 31 October. The fast halo CME associated with this flare transited very rapidly from the Sun to Earth in about 19 hours and drove a new round of extreme geomagnetic activity, leading to additional Kp values of 9_0, a secondary maximum running Ap value of 220, and a secondary enhancement of the provisional Dst to –401.

The X28 flare and fast CME on 4 November were an incredible finale for Region 486 as it transited the West limb. The x-ray flare is very likely the largest observed during the GOES/SMS observing era of the past 28 years and the CME speed of about 2.4×10^3 km/s is truly an extreme. Due to the location of 486 at the time of this event, however, the geophysical consequences at Earth were not as remarkable as the X17 and X10 events. However, had Region 486 been near the center of the solar disk at the time of this event, it is likely that the geophysical consequences would have been exceptional.

A wide range of effects on human activities and technological systems were observed and some of these have been discussed in section 5 of this document. The most extensively reported effects were seen from the interaction of energetic particles with human spacecraft operations and in spacecraft electronics difficulties. We discussed a number of specific deep space missions and near-earth satellites which were affected. Perhaps of greatest significance are the loss of the MARIE instrument on the Mars Odyssey mission and the loss of the ADEOS-2 satellite (which had about development cost of about $640 million). The impact of this interval on airline operations is also particularly noteworthy. Airline routes and schedules were significantly affected because of communication degradation in the daylit and Polar Regions and because of concerns about increased radiation exposure in the Polar Regions.

Although the spacecraft and the airlines effects were most prevalent, it is also clear that a broader range of problems occurred, including HF/VHF communication systems, LF/VLF communications, Global Positioning System (GPS) applications, and electrical power systems. The disruption of electrical power in southern Sweden for about 30 minutes during the activity late on October 30th is certainly a significant example.

What makes this interval of activity particularly noteworthy from a scientific and technical point of view is the diversity of space weather observations which were being made, many of which were not available in the past during similar extreme space weather events. The high levels of geophysical impacts and the wide range of observations will undoubtedly lead to more detailed and extensive analyses of space weather then have been possible in the past. Provided in this document is the important context within which such analyses may be considered.

REFERENCES

Campbell, W. H., *Introduction to Geomagnetic Fields*, Cambridge University Press, New York, 1997.

Delaboudiniere, J-P, *Solar Physics* 162, 291, 1995.

Bruckner, G.E., *Solar Physics* 162, 357, 1995.

Kappenman, J., personal communication, 2003.

Mayaud, P. N., Derivation, Meaning, and Use of Geomagnetic Indices, *American Geophysical Union*, Washington, D. C., 1980.

Skoug, R., personal communication, 2003.

Solar Cycle Number 23 – A Progress Report, R. Thompson, *GPS Solutions*, Vol 6, No. 1-2, 2002, pp 121-123. Springer-Verlag, Berlin.

Sugiura, M., and S. Hendricks, Provisional hourly values of the equatorial Dst for 1961, 1962, and 1963, *NASA Tech. Note D-4047*, 1967.

Zurbuchen , T.H., G. Gloeckler, F. Ipavich, J. Raines, C.W. Smith, L.A. Fisk, On the fast coronal mass ejections in October/November 2003: ACE-SWICS results, unpublished manuscript, 2004.

Zwickl, R.D., K.A. Doggett, S. Sahm, W.P. Barrett, R.N. Grubb, T.R. Detman, V.J. Raben, The NOAA Real-Time Solar-Wind (RSTW) System Using ACE Date, *Space Science Reviews* 86: 633-648, 1998.